

# Effect of Graphene Nanoplatelets (GNPs) on Tribological and Mechanical Behaviors of Polyamide 6 (PA6)

F. Mindivan<sup>a</sup>

<sup>a</sup>Bilecik Seyh Edebali University, Bozuyuk Vocational College, Department of Technical Programs, Bilecik, Turkey.

## Keywords:

Graphene  
Composite  
Polyamide 6  
Scratch hardness  
Tribology

## ABSTRACT

The effects of Graphene Nanoplatelet (GNP) on mechanical and tribological properties of Polyamide 6 (PA6) were studied. The composites were blended using twin-screw extruder and subsequently injection molded for test samples. Mechanical properties were investigated in terms of microhardness, scratch hardness and Young's modulus measurements and tensile test. The tribological behavior of composites was studied by using ball-on-disc reciprocating tribometer. Recent studies showed that the addition of GNP in PA6 matrix resulted in enhancement of mechanical and tribological properties.

## Corresponding author:

Ferda Mindivan  
Bilecik Seyh Edebali University, Bozuyuk  
Vocational College, Department of  
Technical Programs, Bilecik, Turkey.  
E-mail: ferda.mindivan@bilecik.edu.tr

© 2017 Published by Faculty of Engineering

## 1. INTRODUCTION ) - ALIGN LEFT

Strong composite materials based on polymeric matrices are increasingly used in wide range of engineering applications, due to their higher stiffness-to-weight ratio in comparison with metallic materials as well as their enhanced corrosion-resistance. In order to improve their poor surface characteristics, various particles such as carbon nanotubes and boron carbide have been used especially in the recent decade [1,2]. Due to its extraordinary mechanical properties with a reported Young's modulus of 1 TPa and a tensile strength of 130 GPa [3,4], graphene nanoplatelets (GNPs) are an ideal reinforcement for strengthening polymer matrices. In order to improve the properties of GNP-polymer

composite, the surface of GNPs is modified either physically or chemically [5]. It is generally considered that the surface modification of GNPs is beneficial to improve the dispersal property of GNPs in polymer matrix. However, the modifying process is usually complicated and damages the structure of the GNPs and thereby greatly reduces their mechanical properties [6]. Thus, the enhancement effect of the GNPs will be weakened.

The objective of this paper is to fabricate PA6/GNP composites and investigate the effects of GNP loading content on the mechanical and tribological properties of the PA6/GNP composites without using any surface modification process.

## 2. EXPERIMENTAL METHODS

GNPs in this study were GRAFEN-IGP2 nanoplatelets (Grafen Chemical Industries, Turkey). These nanoparticles consist of short stacks of graphene layers having a lateral dimension of ~5 nm and a thickness of ~5–8 nm. SEM observation (Fig. 1) of GNPs shows that the GNPs superimpose together and look like wrinkled or crumpled thin paper. Melt blending of PA6 and GNP was carried out in a co-rotating twin screw extruder (Thermoprism TSE 16 TC, L/D 24) at a screw speed of 100 rpm and barrel temperature profile of 230-230-230-230-230 °C, followed by granulation (3–5 mm long and 3 mm in diameter) in a pelletiser and drying. Prior to extrusion, the PA6 polymer and GNP were dehumidified in a vacuum oven at 90 °C for a period of 24 h. The GNP content in the PA6/GNP composites was varied from 1 – 4 wt.% (Table 1). The composite mixture was molded using a laboratory scale plunger type injection-molding machine (Micro injector, Daca Instruments) at a barrel temperature of 200 °C and mold temperature of 30 °C, for preparation of microhardness, scratch hardness, Young's modulus, tensile and tribological test samples.

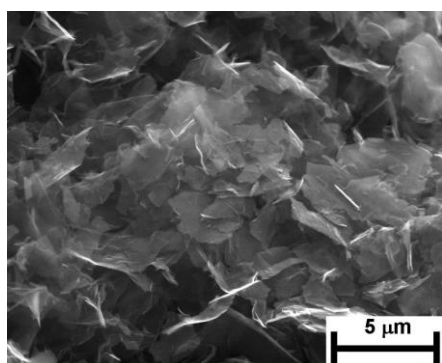


**Fig. 1.** The SEM image of GNPs.

**Table 1.** Ratios and codes of GNP in the composites.

Samples	GN Content (in weight %)
PA6/GNP-1	1
PA6/GNP-2	2
PA6/GNP-4	4

Room temperature mechanical properties of the unfilled PA6 and PA6/GNP composites were determined according to microhardness and Young's modulus measurements, scratch hardness and tensile tests. Microhardness measurement was carried out on metallographic samples under the load of 50 g with a Vickers indenter. At least ten successive measurements

were performed for each condition. The Impulse Excitation Technique (IET) was used to measure the Young's modulus of the sample series in accordance with the ASTM E 1876 standard [7]. Briefly, IET utilises the phenomenon of free mechanical resonance of flexural vibrations when these vibrations are excited by tapping the test sample. Analysis of the fundamental frequency of a specific vibration mode, which depends on sample mass, stiffness, and geometry, allows determining the Young's modulus by measuring the resonance frequency. The tensile test samples with a gage length of 80 mm were also tested according to the ASTM D 3822 standard [8] on Lloyd LR 5K tensile testing machine with a load cell of 10 N and the deformation rate was 20 mm/min. All the results represented an average value of five tests with standard deviations. The scratch tester, designed and built in our laboratory, was used to carry out scratch tests equipped with a Rockwell C-type conical indenter under laboratory environment condition (the temperature was 25 °C and the humidity was ~30-35 % RH). The tests were conducted at four different loads (5, 10, 15 and 20 N) with a constant tip velocity of 0,007 m/s. The length of the scratch was kept constant as 10 mm. In order to assess tribological properties of the unfilled PA6 and PA6/GNP composites, the friction and wear tests were conducted on a reciprocating wear tester under dry sliding conditions. The ambient temperature was approximately 25 °C and the relative humidity was nearly 40 ±5 %. The wear tests on all samples were performed under a constant load of 10 N using a 10 mm diameter 304 steel ball at a sliding velocity of 1.7 cm s<sup>-1</sup>. In all tests, the total sliding distance was kept constant at 50 m. The wear was calculated by analysing width and depth of wear scars developing on sample surfaces with the help of a contact stylus profilometer (SJ400). Following the wear tests, the steel counterface surfaces were examined under an Optical Microscope (OM) in order to investigate the wear mechanisms. Then, scratch and wear scars on the surfaces of the unfilled PP and PA6/GNP composites were examined using a Scanning Electron Microscope (SEM- Carl Zeiss AG - SUPRA 40).

## 3. RESULTS AND DISCUSSION

Figure 2 showed XRD patterns of the unfilled PA6 and PA6/GNP composites. PA6 exhibited

polymorphic structures containing two types of crystal form: monoclinic ( $\alpha$ ) and pseudo-hexagonal ( $\gamma$ ). The representative diffraction peaks observed at  $2\theta=20.4^\circ$  and  $21.8^\circ$  corresponded to  $\alpha$  and  $\gamma$  crystalline phases of the unfilled PA6 [9,10], respectively. As shown in Fig. 2,  $\alpha$  phase was the dominant crystalline phase for the unfilled PA6. Also, all composites showed two peaks at  $2\theta=20.1^\circ$  and  $22.1^\circ$ , corresponding to  $\alpha$  and  $\gamma$  crystalline phases. When compared to the unfilled PA6, the diffraction peak corresponding to  $\alpha$ -form crystal phase was observed only as a less pronounced shoulder at all GNP contents. However, the peak of  $\gamma$  form crystal phase in the PA6/GNP composites grew more obvious. However, referring to Fig. 2, in addition to the two reflections as seen in the PA6/GNP composites a other reflection was also detected at  $2\theta=26^\circ$  which was related to the GNP [11]. According to these results, GNPs changed crystal structure of all composites. Gong et al. [12] reported that the diffraction peaks of  $\alpha$ -form crystals of modified graphene based PA6 composites become weaker with an increase of GNP loading content. Oneill et al. [3] showed that functionalized graphene oxide (GO) and functionalized reduced graphene oxide (rGO) could promote the formation of  $\gamma$  phase crystals in the PA6 matrix.

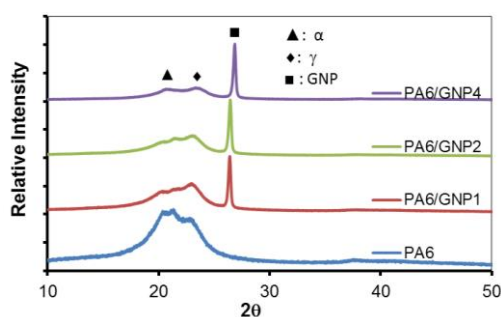


**Fig. 2.** XRD patterns of unfilled PA6 and PA6/GNP composites.

The mechanical properties of PA6/GNP composites are characterized by their tensile strength, Young's modulus, elongation at break and microhardness. The effects of GNP loading content on tensile strength and Young's modulus of the composites are displayed in Fig. 3. As shown in Fig. 3, the PA6/GNP composites show similar tensile strength compared to that of unfilled PA6. In addition, the Young's modulus of PA6/GNP composites increases with an increase in GNP contents (Fig. 3). The Young's modulus of the composite with 4 wt.% loading content of GNPs increased by 50 %, compared with that of unfilled PA6.

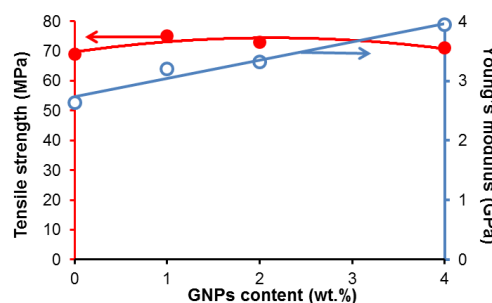


**Fig. 3.** Tensile strength and Young's modulus of PA6 filled with various contents of GNPs.

The influences of GNP loading content on elongation at break and microhardness of the composites are presented in Fig. 4. As seen from Fig. 4, the elongation at break of the composite decreases with an increase of GNP loading content and when the loading content is 4 wt.%, the value decreases by 95 % in comparison with that of unfilled PA6. However, the microhardness of composite increases with an increase of GNP loading content and when the loading content is 4 wt.%, the value increases by 38 % in contrast to that of unfilled PA6. The results of mechanical properties revealed that the incorporation of GNPs could improve the strength, but increase brittleness in the PA6/GNP composites due to alteration of the crystal structure of the PA6 matrix by the GNP (Fig. 2). Chatterjee et al. [6] reported that nanofillers could affect the mechanical properties of PA matrix by changing the crystallinity, which seems to be in compatible with my results.

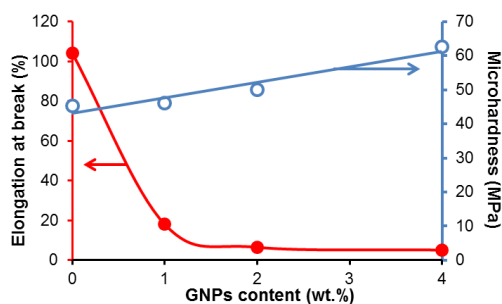


**Fig. 4.** Elongation at break and microhardness of PA6 filled with various contents of GNPs.

In Fig. 5, by increasing the GNP content, scratch hardness showed a rising trend because of the existence of GNPs in the direction of the scratch test (Fig. 6) and decreased with increasing applied load. The rise of scratch hardness at a load of 20 N was sharper than the rise of the scratch hardness at lower loads (5, 10 and 15 N) because the role of the GNPs was diminished at smaller scratch depths.

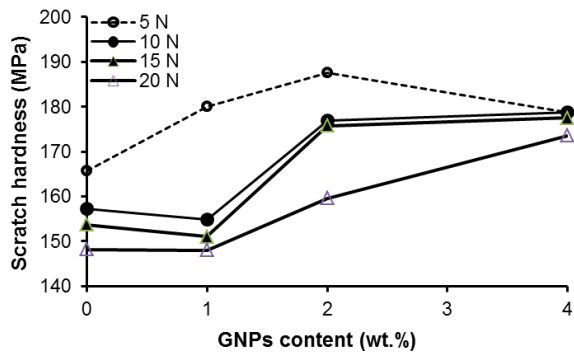
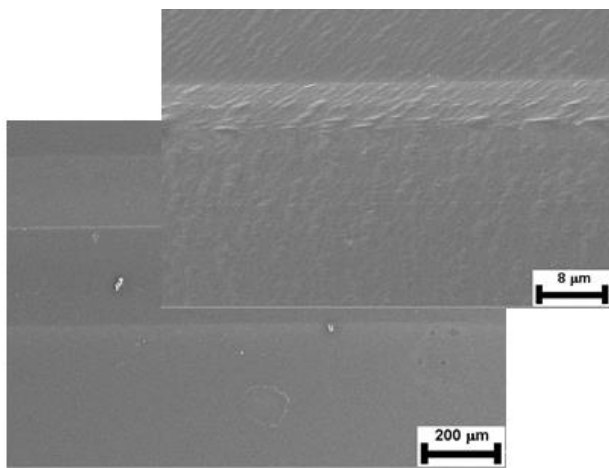
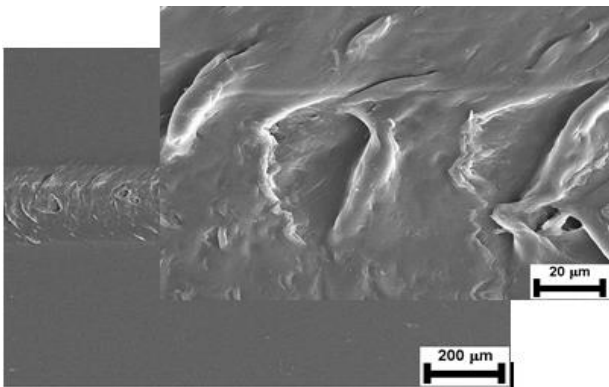


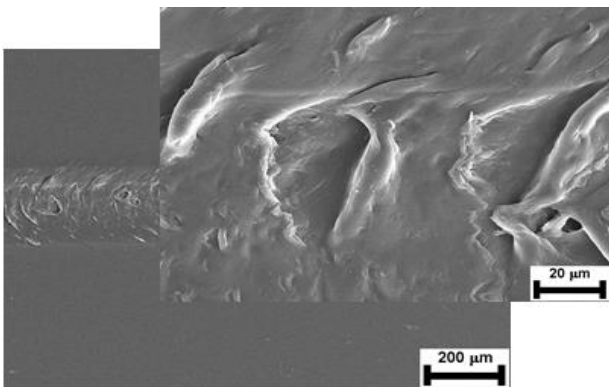
Fig. 5. Scratch hardness of PA6 filled with various contents of GNPs.



(a)



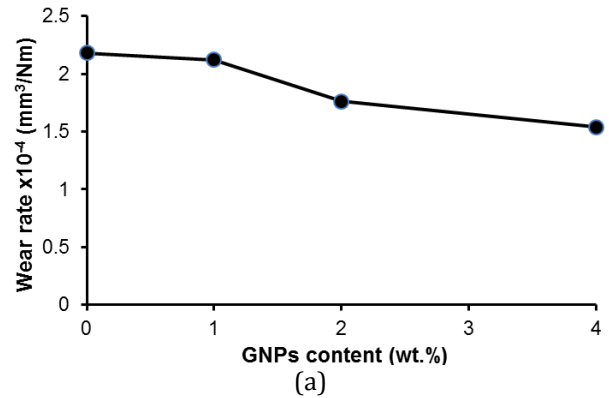
(b)



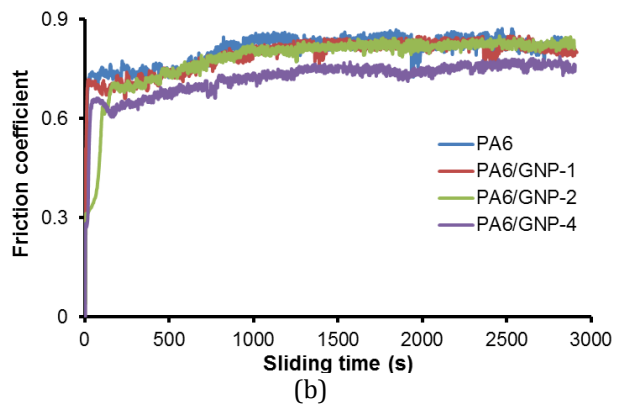
(c)

Fig. 6. Low and high magnification SEM micrographs of scratch scars generated on the (a) unfilled PA6, (b)

2 wt.% PA6/GNP-2 composite and (c) 4 wt.% PA6/GNP-4 composite at a load of 20 N.



(a)



(b)

Fig. 7. (a) Wear rate and (b) friction coefficient of PA6 filled with various contents of GNPs.

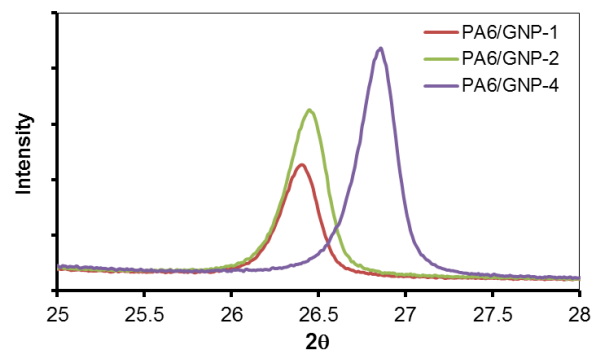
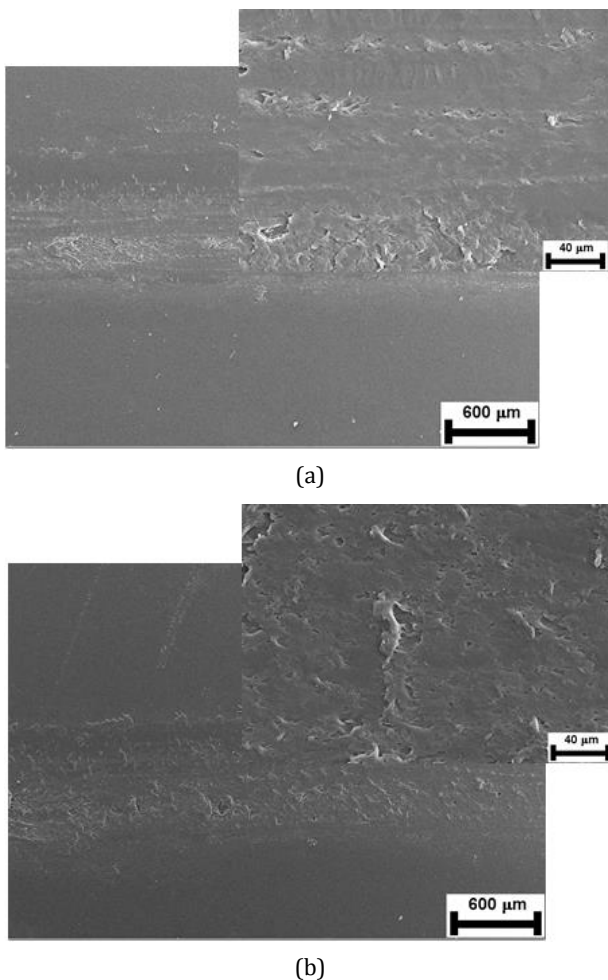


Fig. 8. Comparison of GNPs' XRD Bragg peak at  $2\theta \sim 26.5$  deg, confirming morphological differences of the composites containing 1, 2 and 4 wt.% of GNP.

The effect of GNP addition on the tribological behavior of PA6 was investigated. It is shown that at small amounts of GNP, wear was reduced (Fig. 7) with a slight decrease in the average friction coefficient (from  $\sim 0.83$  in the unfilled PA6 to 0.74 in the composite with 4 wt.% of GNP-4). Moreover, a larger number of graphene sheets were obtained by adding more GNP into the PA6 matrix as illustrated in Fig. 8. A small increase in the basal spacing (the peak was shifted to the right) was also noted for the

composites containing more GNP. These differences probably affected the tribological behavior. It should be noted that the van der Waals forces in the composite with 4 wt.% of GNP-4 would have been lower than in the other composites, which could lead to a much easier way for the GNP layers to slide over each other.

The SEM images of wear tracks for the unfilled PA6 and the composite with 4 wt.% of GNP-4 shown in Fig. 9 (all at the same magnification) are in accordance with the above analysis. For the unfilled PA6, the worn surface is rough and exhibits some scratch grooves parallel to the sliding direction in the worn surface when sliding against the steel counterface. From the image of the composite with 4 wt.% of GNP-4, it can be seen that nonuniform thin sheets are generated in the whole area investigated and thereby a rippled structure is formed, which is perpendicular to the sliding direction.



**Fig. 9.** Low and high magnification SEM micrographs of wear tracks generated on the (a) unfilled PA6, and (b) 4 wt.% PA6/GNP-4 composite.

Figure 10 shows OM images of the steel counter balls sliding against the unfilled PA6 and the composite with 4 wt.% of GNP after a sliding distance of 50 m. The rod like wear particles from the PA6 to the counter surface are white and adhere to the counter steel surface due to serious oxidization (Fig. 10a). It is evident that the temperature at the sliding interface has reached its melting point of PA6 during sliding, resulting in a poor wear property. On the other hand, some GNP particles reducing the friction by providing interfacial sliding between the surface and steel counter ball were observed on steel ball surface sliding against the composite with 4 wt.% of GNP (Fig. 10b). Dike et al. [1] have reported similar observations with CNTs in a polypropylene (PP) matrix and proposed that these fillers diminish the adhesion between the matrix and the counter surface; the digging phenomenon is thus reduced, and this results in a relatively higher wear resistance.

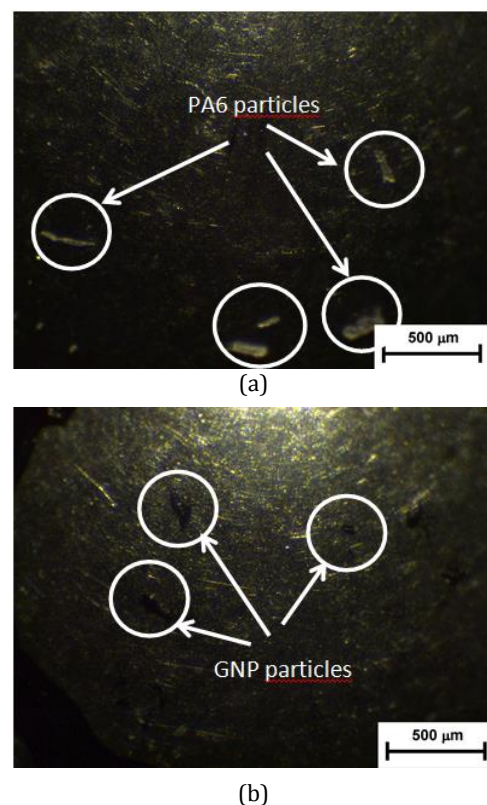


**Fig. 10.** OM images of the steel balls sliding against the (a) unfilled PA and (b) composite with 4 wt.% of GNP.

#### 4. CONCLUSIONS

The addition of GNP has been proven an effective way to improve the Young's modulus, microhardness, scratch hardness and

tribological performance of PA6-based polymer matrix without necessarily compromising tensile strength.

### Acknowledgement

The author thanks the financial support of the research foundation (Project no.: 2014-01.BIL.07-01) of Bilecik Seyh Edebali University.

### REFERENCES

- [1] A.S. Dike, F. Mindivan and H. Mindivan, 'Mechanical and tribological performances of polypropylene composites containing multi-walled carbon nanotubes', *International Journal of Surface Science and Engineering*, vol. 8, no. 4, pp. 292-301, 2014.
- [2] A.S. Dike, F. Mindivan and H. Mindivan, 'Effect of B<sub>4</sub>C content on the mechanical and tribological performances of polypropylene', *Acta Physica Polonica A*, vol. 125, pp. 396-398, 2014.
- [3] A. O'Neill, D. Bakirtzis and D. Dixon, 'Polyamide 6/Graphene composites: The effect of in situ polymerisation on the structure and properties of grapheme oxide and reduced graphene oxide', *European Polymer Journal*, vol. 59, pp. 353-362, 2014.
- [4] J.A. Puértolas and S.M. Kurtz, 'Evaluation of carbon nanotubes and graphene as reinforcements for UHMWPE-based composites in arthroplastic applications: A review', *Journal of the Mechanical Behavior of Biomedical Materials*, vol.39, pp. 129-145, 2014.
- [5] Y. Song, J. Yu, L. Yu, F.E. Alam, W. Dai, C. Li and N. Jiang, 'Enhancing the thermal, electrical, and mechanical properties of silicone rubber by addition of graphene nanoplatelets', *Materials and Design*, vol. 88, pp. 950-957, 2015.
- [6] S. Chatterjee, F.A. Nüesch and B.T.T. Chu, 'Crystalline and tensile properties of carbon nanotube and graphene reinforced polyamide 12 fibers', *Chemical Physics Letters*, vol. 557, pp. 92-96, 2013.
- [7] ASTM E 1876, Standard test method for dynamic young's modulus, shear modulus, and poisson's ratio by impulse excitation of vibration, American Society for Testing and Materials, 2001.
- [8] ASTM D 3822, Standard test method for tensile properties of single textile fibers, American Society for Testing and Materials, 1997.
- [9] T. Kashiwagi, R.H. Harris Jr, X. Zhang, R.M. Briber, B.H. Cipriano, S.R. Raghavan, W.H. Awad and J.R. Shields, 'Flame retardant mechanism of polyamide 6-clay nanocomposites', *Polymer*, vol. 45, pp. 881-891, 2004.
- [10] P. Ding, S. Su, N. Song, S. Tang, Y. Liu and L. Shi, 'Highly thermal conductive composites with polyamide-6 covalently-grafted graphene by an in situ polymerization and thermal reduction process', *Carbon*, vol. 66, pp. 576-584, 2014.
- [11] J. Ma, Q. Meng, I. Zaman, S. Zhu, A. Michelmore, N. Kawashima, C.H. Wang and H.-C. Kuan, 'Development of polymer composites using modified, high-structural integrity graphene platelets', *Composites Science and Technology*, vol. 91, pp. 82-90, 2014.
- [12] L. Gong, B. Yin, L.-P. Li and M.-B. Yang, 'Nylon-6/Graphene composites modified through polymeric modification of graphene', *Composites: Part B*, vol. 73, pp. 49-56, 2015.